Annals of Nuclear Medicine Vol. 6, No. 3, 153–158, 1992

Correction of scattered photons in Tc-99m imaging by means of a photopeak dual-energy window acquisition

Akihiro KOJIMA,* Akinori TSUJI,* Yoshikazu TAKAKI,* Seiji TOMIGUCHI,* Masafumi HARA,* Masanori MATSUMOTO** and MUTSUMASA TAKAHASHI*

*Department of Radiology, Kumamoto University School of Medicine
**Department of Radiological Technology, College of Medical Science, Kumamoto University

We are proposing a new method for correcting of scattered photons in technetium-99m (^{99m}Tc) imaging by means of photopeak dual-energy window acquisition. This method consists of the simultaneous acquisition of two images and estimation of a scatter image included in the symmetric energy window (SW) image by the difference between these images. The scatter corrected image is obtained by subtracting the scatter image from the SW image. In order to evaluate this method, we imaged a planar and a SPECT phantom with cold lesions and calculated the contrast value with and without the scatter correction. In addition, we performed asymmetric energy window (ASW) imaging to compare with this scatter correction method for planar images. In the planar image with the tissue-equivalent material of 10 cm, the scatter correction method removed 32% of the counting rate of the SW image and improved from 0.81 to 0.94 of the contrast value for a 4 cm-diameter cold lesion, while the contrast value with the ASW was 0.87 for such a cold lesion. The scatter corrected SPECT image had a reduction of 18% of the counting rate of the SW SPECT image and improvement of ~11% in contrast for cold spot sizes larger than a 3 cm-diameter, compared with the SW SPECT image. In addition, a perfusion defect could be well visualized by this scatter correction method on ^{99m}Tc-HMPAO regional cerebral blood flow SPECT of a patient. Our proposed scatter correction method can improve both planar and SPECT images qualitatively and quantitatively.

Key words: Compton scatter correction, photopeak dual-energy window acquisition, scatter image

INTRODUCTION

GAMMA RAYS ARISING FROM THE SOURCES that are distributed in the body are scattered by the tissue. These scattered photons are sometimes used to estimate the depth of the source with the planar images[1] and depict the body contour in single photon emission computed tomography (SPECT).[2] However, since scattered photons included in the image acquired with the conventional photopeak energy window degrade the image quality, they must be removed from such an image for quantification of radioactivity.

Many scatter correction methods have been proposed and evaluated in various phantom experiments and clinical studies.[3–8] Recently, the energy weighted acquisition (EWA) technique with an online weighted acquisition module (WAM) has been developed and used in various radionuclide imaging.[9]

We have developed a new method to remove scattered photons within the conventional photopeak window by means of the photopeak dual-energy window acquisition technique. The purpose of this study is to evaluate this new scatter correction method for technetium-99m (^{99m}Tc) imaging on phantom experiments and a clinical study.

Received November 6, 1991, revision accepted February 21, 1992.

For reprints contact: Akihiro Kojima, M.Sc., Department of Radiology, Kumamoto University School of Medicine, 1–1–1, Honjo, Kumamoto 860, Japan.

THEORY

The limited energy resolution of a gamma camera causes inclusion of scattered photons within the photopeak energy window. The content of scattered photons is investigated through the Monte Carlo simulations and the phantom experiments with respect to energy and spatial distributions.[10–13] Our experimental data demonstrated that most of scattered photons within the symmetric energy window (SW) set on the photopeak of ^{99m}Tc were included in the lower half of the SW (75%–80%).[13] On the basis of this result, we have performed the following scatter correction;

(1) setting of two energy windows on the primary photopeak of ^{99m}Tc: the lower energy window (LEW: 126–140 keV) and the upper energy window (UEW: 140–150 keV),
(2) simultaneous acquisition of the image I_L with the LEW and the image I_U with the UEW,
(3) correction of field-uniformity for these two images: the uniformity-corrected images I_{LU} and I_{UU},
(4) estimation of a scatter image I_S by subtracting image I_{UU} from image I_{LU},
(5) calculation of a scatter corrected image I_{SC} by subtracting image I_S' processed by a smoothing filter from the SW image ($I_{LU}+I_{UU}$).

The above procedures are schematically illustrated in Fig. 1.

MATERIALS AND METHODS

A dual-head gamma camera with two low energy high resolution collimators (GCA 90B-E2, Toshiba) was used in this study. Dual-energy window acquisition was possible for either of two heads. The field of view of the camera was rectangular (50 cm × 35 cm) and one pixel size was 1 mm for a 512 × 512 matrix. The energy resolution of the gamma camera was 13% for 140 keV. The acquired data were processed by means of an on-line computer (GMS 550U, Toshiba). For the dual-energy window (DEW) method, the two energy windows (LEW: 126–140 keV and UEW: 140–154 keV) were set on the photopeak of ^{99m}Tc. Moreover, the asymmetric energy window (ASW: 133–154 keV) method was also employed to compare with the DEW method.

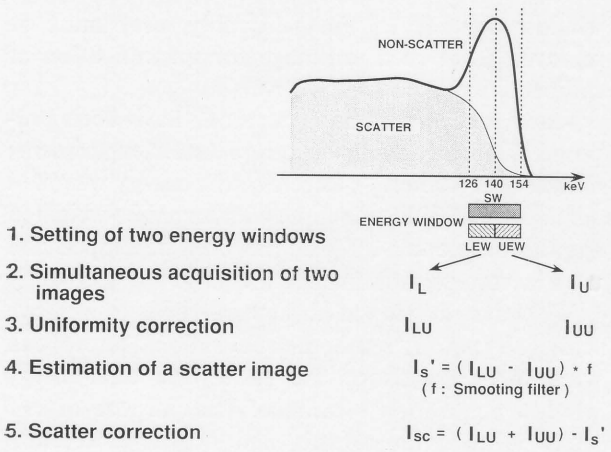

Fig. 1 Illustration of the scatter correction method using two energy windows set on a photopeak.

Experimental studies for planar images

An IAEA liver plate phantom (ILS type, Kyoto kagaku) was used for the planar images. The phantom was made of acrylate and had a thickness of 1 cm and a volume of 215 m*l* with eight cold lesions (0.8, 1, 1.2, 1.6, 2, 2.5, 3, and 4 cm in diameter). This phantom, filled with water containing 100 MBq of ^{99m}Tc, was placed 10 cm from and parallel to the camera face. In order to change the content of scattered photons, plates of tissue equivalent material (Tough water, WE type, Kyoto kagaku, 30 cm × 30 cm × 2 cm-thick) were inserted between the source and the camera, and increased in thickness from 0 to 10 cm in 2 cm increments. The planar images with 2 million counts were acquired in a 256 × 256 frame mode for the DEW method and the ASW method.

All data acquired with the asymmetric energy windows (LEW, UEW, and ASW) were corrected with the flood data (about 30 million counts) collected within the same energy windows for field-uniformity. The SW images were obtained as the addition of the uniformity corrected LEW and UEW images. In order to reduce high frequency noise in the raw scatter image I_S, a twenty-five (5 × 5) points weighted smoothing filter (GMS 550U software series, Toshiba) was applied to image I_S in the object domain through a convolution operation.

For three cold lesions (1.6, 2, and 4 cm) on planar images, the contrast value CV was calculated by the following equation;

$$CV=\frac{C_{BG}-C_D}{C_{BG}} \quad (1)$$

where C_D was the counts/pixel for a region of interest (ROI) (3 × 3 pixels) placed in the center of the defect and C_{BG} was the counts/pixel for an ROI (9 × 9 pixels) set on the background near these defects.

Experimental studies for SPECT images

A phantom with eight cylinders (0.5, 1, 1.5, 2, 2.5, 3, 3.5, and 4 cm in diameter) was employed for SPECT data acquisition. This phantom was filled with non-radioactive water and placed in a cylinder (20 cm in diameter and 20 cm in length) filled with water containing 74 kBq/m*l* of ^{99m}Tc to obtain SPECT images

with cold spots. The projected images were acquired with 60 angular steps over 360° at 20 sec per view, with 1.5× magnification and a 128×128 matrix. The central axis of the outer cylinder was on the camera rotation axis and the radius of rotation was 20 cm.

Two projection data sets were acquired with the LEW and UEW, simultaneously. After uniformity correction for each data set, two projection image sets were obtained with and without scatter correction. Transverse slices with a thickness of 3 pixels (1 pixel size=2.7 mm) were reconstructed by the filtered backprojection, using a Shepp and Logan filter. The attenuation correction by the Chang method was performed with an attenuation coefficient of 0.12 cm^{-1} for images with the scatter correction and 0.10 cm^{-1} for images without it. These values for making the correction matrix were chosen as the values producing relatively uniform transaxial images of a cylindrical phantom.

The contrast values were also calculated for each cold lesion using Eq. (1).

Clinical study

We applied our scatter correction method to the ^{99m}Tc-HMPAO SPECT of a patient with anterior cerebral contusion. Projection images were acquired in 128×128 matrix with 1.5× magnification and a 28 cm radius of rotation 30 min after i.v. injection of 740 MBq ^{99m}Tc-HMPAO. Sixty images were obtained over 360° at 30 sec per view. Transverse images with 4 pixels-thickness were reconstructed with the same procedures as the phantom.

RESULTS

Planar images

Figure 2 shows two planar images acquired simultaneously with the photopeak dual-energy window technique and an estimated scatter image. The thickness of the scattering material was 10 cm. The total counts for the LEW and UEW image were 1.34×10^6 and 0.67×10^6, respectively. It is apparent that the LEW image has more scattered photons than the UEW image. Consequently, on the LEW image, contrasts were degraded in each defect and the peripheral edge of the phantom was not sharp. The scatter image estimated was an extremely blurred image and had totals of 0.65×10^6 counts.

Images obtained by the different energy window techniques are shown in Fig. 3. As true data, an image acquired with the SW in air is also shown. The images by the SW and ASW had worse contrast and more scattered photons around the phantom images. Although the scatter corrected image lost 32% of the counting rate of the SW image due to subtraction of the scatter image, it had improved

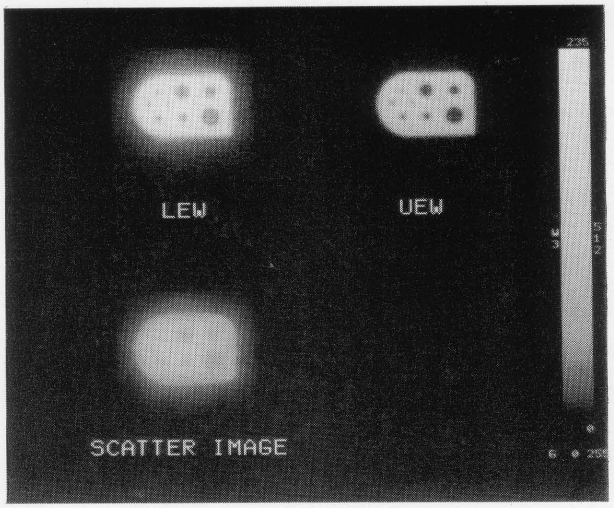

Fig. 2 Planar images of a liver phantom with field-uniformity correction, acquired with a LEW and a UEW. A scatter image was obtained by smoothing an image after subtracting the UEW image from the LEW image. The thickness of the scattering material was 10 cm.

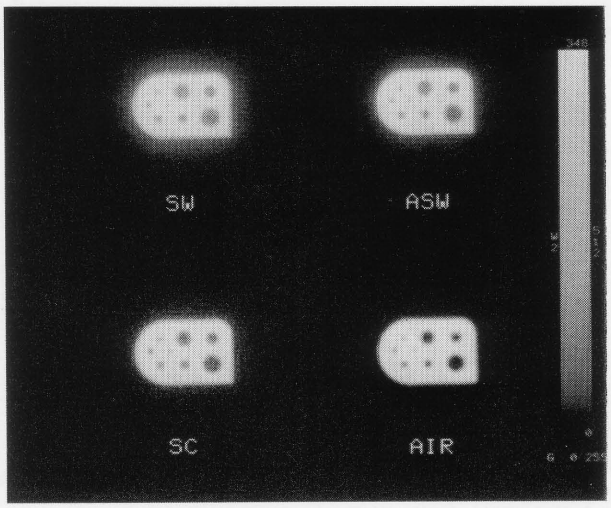

Fig. 3 Planar images of a liver phantom obtained with the symmetric energy window (SW), asymmetric energy window (ASW), and scatter correction (SC) method. The thickness of the scattering material was 10 cm. An image in air (AIR) is shown as a reference image.

contrast for each lesion and became similar to the image in air. The contrast values in each cold lesion are plotted against the thickness of the scattering material in Fig. 4. These values decreased linearly as thickness increased. However, the contrast values for the larger cold lesions were greatly improved with the scatter corrected method in the thicker materials. For a defect size of 1.6 cm, the beginning from low contrast values at a thickness of 0 cm were due to the limited spatial resolution of the gamma camera. The contrast values for three cold lesions in three images at a thickness of 10 cm are listed in Table 1.

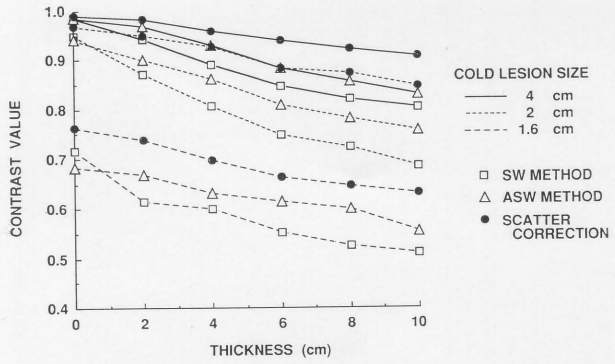

Fig. 4 Contrast value vs thickness of scattering material for three cold lesions in planar images. Three imaging techniques are compared.

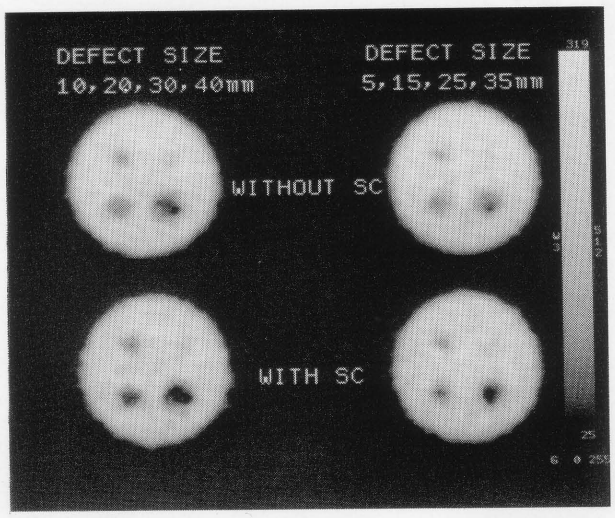

Fig. 5 SPECT images of a phantom with cold lesions (5–40 mm) with and without scatter correction (SC) method.

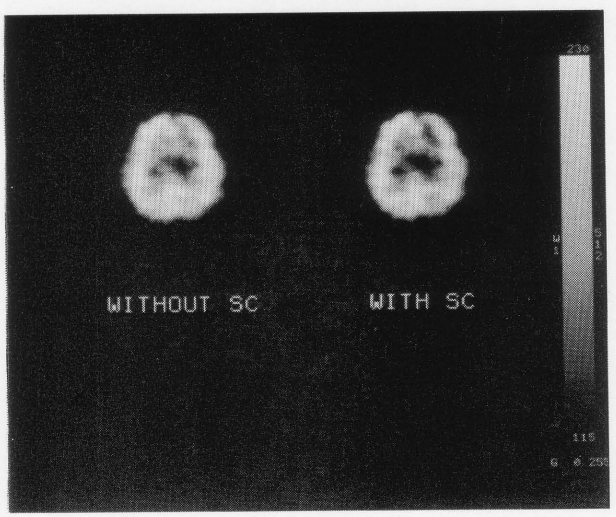

Fig. 6 SPECT images with and without scatter correction (SC) method in ^{99m}Tc-HMPAO r-CBF study for a patient with contusion of the left frontal lobe.

Table 1 Comparison of contrast values for cold lesions in planar images

Cold spot size (mm)	Contrast value* (error**)			
	SW	ASW	SC	AIR
16	0.65 (25.3%)	0.72 (17.2%)	0.83 (4.6%)	0.87
20	0.70 (24.7%)	0.80 (14.0%)	0.90 (3.2%)	0.93
40	0.81 (17.3%)	0.87 (11.2%)	0.94 (4.1%)	0.98

SW: 20% symmetric energy window (10 cm scattering material), ASW: 15% asymmetric energy window 10 cm scattering material), SC: scatter correction (10 cm scattering material), AIR: 20% symmetric window (air).

* contrast value=$(C_{BG}-C_D)/C_{BG}$

** error from AIR data

Table 2 Comparison of contrast values for cold lesions in SPECT images

Diameter (mm)	Contrast value*		Improvement (%)
	Without SC	With SC	
5	0.152	0.155	2.3
10	0.257	0.270	5.0
15	0.497	0.537	8.0
20	0.624	0.662	6.1
25	0.685	0.738	7.7
30	0.707	0.786	11.2
35	0.763	0.856	12.2
40	0.847	0.928	9.6

SC: scatter correction

* Contrast value: $(C_{BG}-C_D)/C_{BG}$

The contrast values in the scatter corrected images differed from the true values in air by 4%.

SPECT images

SPECT images with eight cold lesions are shown in Fig. 5 with and without the scatter correction. Improvements in contrast in larger cold lesions could be seen on the scatter corrected images. However, the scatter corrected SPECT images had the total counts of 82% of the original SPECT image due to the subtraction of the scatter image. Table 2 lists contrast values with and without the scatter correction for all cold lesions. About 11% improvement in the image contrast was seen for larger cold lesions.

Clinical SPECT images

Figure 6 shows the comparison of regional cerebral blood flow SPECT images of a patient with anterior cerebral contusion using ^{99m}Tc-HMPAO. The image with the scatter correction defined the decreased perfusion in the left frontal region to better advantage than without the scatter correction.

DISCUSSION

Scintigraphic images are obtained by the energy window set on a photopeak. Since photons which are scattered in a small angle are included within this window due to the poor energy resolution of the gamma camera, these degrade image quality. Several methods to remove these scattered photons have therefore been developed.[4,5,14,15] Simple techniques used in removing scattered photons in images are to employ a narrow symmetric energy window or an asymmetric energy window. However, these techniques remove not only scattered photons but also non-scattered photons because they raise the lower threshold of the energy window. Therefore, the imaging time is prolonged to compensate for the decreased count-rate of non-scattered photons.[4] Other methods remove scattered photons from SPECT images by a convolution or a deconvolution technique.[14,15] In these methods the scatter image was assumed to be the convolution of the total (scatter+non-scatter) images[14] or non-scatter images[15] with an exponential function. The parameters of such a function were estimated experimentally[14] or mathematically[15] (Monte Carlo simulation). However, it is difficult to determine the optimum parameters for various routine clinical studies in these convolution techniques. Jaszczak et al.[5] developed a method to compensate for scattered photons in SPECT images by means of a dual-energy window acquisition. They estimated a scatter image by multiplying a normalized factor "k" by an image acquired with an energy window set on a Compton scattering region. The value for k was found to be 0.5 experimentally and mathematically. This method made possible the quantitatively accurate results in their studies. However, a constant value of k cannot be uniquely determined for many clinical situations. Recently, the selection of k has been investigated.[6–8]

Recently, a new scatter rejection technique by means of energy-weighted acquisition (EWA) has been developed.[9] This method can obtain the scatter corrected data online without post-processing and is applicable to imaging with various nuclides. Halama et al.[9] reported that there was a contrast improvement of about 40% for gallium-67 and thallium-201, and 18% for ^{99m}Tc. However, it has the following drawbacks: the EWA is equipped with the only one energy weighting function for a nuclide and requires a special electric device called a "weighted-acquisition module (WAM)."

We developed a new scatter correction method with the photopeak dual-energy window technique. This method is unlike the method proposed by Jaszczak et al.[5] with regard to setting the two energy windows and estimating a scatter image. In our method, the symmetric energy window (SW) set on the photopeak (140 keV$\pm$10%) is divided into two equal regions and the scatter image is made by subtracting the upper window image from the lower window image. This is based on the fact that most scattered photons within the SW are included in the lower half of the SW. From our previous study, we confirmed that these inclusions were 75%–80% when the thickness of the scattering material was changed from 2 to 20 cm.[13] Therefore, although a few scattered photons remain in the scatter-corrected image, our method which uses the upper window image is not greatly affected by the distribution of the radioactive source.

SPECT is often employed to accurately quantitate the distribution of radioactivity in the body. However, there are some problems in this quantification. In our previous work, we reported the effect of the spatial resolution on SPECT values.[16] Although SPECT values represented the true radioactivity at the hot spot size larger than 2.5–3$\times$(the spatial resolution of the gamma camera), these had errors of about 20% for the cold spot lesions with such sizes. This was mainly due to scattered photons. It is also important to perform accurate attenuation correction. The generally used attenuation correction methods employ the attenuation coefficient that is empirically determined according to the number of scattered photons. In this study we used attenuation coefficients of 0.12 cm^{-1} and 0.10 cm^{-1} for SPECT images with and without the scatter correction, respectively. These values were experimentally determined as the values which gave flat transaxial images for a uniform cylindrical source. We compared the contrast values in cold spots in these attenuation corrected SPECT images. This evaluation was similar to the study by Halama et al.[9] Although with the scatter correction the value of the attenuation coefficient was greater, it was smaller than the true value (0.15 cm^{-1}). We think that this result was due to the scattered photons remaining within the scatter corrected images and the performance of the attenuation correction method used. If the scatter correction is performed perfectly, it is possible to correct the attenuation with the true attenuation coefficient for a uniformly scattering material.

Our method is to apply to a gamma camera with a dual-energy window acquisition mode. However, it is important to accurately perform the field-uniformity correction for the raw data because our method requires two images with extremely asymmetrical energy windows. At present usefulness of our method for the scintigraphic imaging is being evaluated in phantom experiments and clinical studies.

CONCLUSIONS

Recently, many ^{99m}Tc labeled radiopharmaceuticals for imaging have been developed and widely used in clinical studies. A new scatter correction method, using two energy windows set on a photopeak, can remove scattered photons from ^{99m}Tc images. This method is applicable to a gamma camera with a dual-energy window acquisition mode and may improve both clinical image quality and quantification.

REFERENCES

1. Filipow LJ, Macey DJ, Munro TR: The measurement of the depth of a point source of a radioisotope from gamma ray spectra. *Phys Med Biol* 24: 341–352, 1979
2. Macey DJ, DeNardo GL, DeNardo SJ: Comparison of three boundary detection methods for SPECT using Compton scattered photons. *J Nucl Med* 29: 203–207, 1988
3. Heller SL, Goodwin PN: SPECT instrumentation: performance, lesion detection, and recent innovations. *Semin Nucl Med* 17: 184–199, 1987
4. Bloch P, Sanders T: Reduction of the effects of scattered radiation on a sodium iodide imaging system. *J Nucl Med* 14: 67–72, 1973
5. Jaszczak RJ, Greer KL, Floyd CE, et al: Improved SPECT quantification using compensation for scattered photons. *J Nucl Med* 25: 893–900, 1984
6. Gilardi MC, Bettinardi V, Todd-Pokropek A, et al: Assessment and comparison of three scatter correction techniques in single photon emission computed tomography. *J Nucl Med* 29: 1971–1979, 1988
7. Mas J, Ben Younes R, Bidet R: Improvement of quantification in SPECT studies by scatter and attenuation compensation. *Eur J Nucl Med* 15: 351–356, 1989
8. Koral KF, Swailem FM, Buchbinder S, et al: SPECT dual-energy-window Compton correction: scatter multiplier required for quantification. *J Nucl Med* 31: 90–98, 1990
9. Halama JR, Henkin RE, Friend LE: Gamma camera radionuclide images: improved contrast with energy-weighted acquisition. *Radiology* 169: 533–538, 1988
10. Floyd CE, Jaszczak RJ, Harris CC, et al: Energy and spatial distribution of multiple order Compton scatter in SPECT: a Monte Carlo investigation. *Phys Med Biol* 29: 1217–1230, 1984
11. Rosenthal MS, Henry LJ: Scattering in uniform media. *Phys Med Biol* 35: 265–274, 1990
12. Ogawa K, Harata Y, Ichihara T, et al: Estimation of scatter component in SPECT planar image using a Monte Carlo method. *Jpn J Nucl Med* 27: 467–476, 1990
13. Kojima A, Matsumoto M, Takahashi M: Experimental analysis of scattered photons in a ^{99m}Tc imaging with a gamma camera. *Ann Nucl Med* 5: 139–144, 1991
14. Axelsson B, Msaki P, Israelsson A: Subtraction of Compton-scattered photons in single-photon emission computerized tomography. *J Nucl Med* 25: 490–494, 1984
15. Floyd CE, Jaszczak RJ, Greer KL, et al: Deconvolution of Compton scatter in SPECT. *J Nucl Med* 26: 403–408, 1985
16. Kojima A, Matsumoto M, Takahashi M, et al: Effect of spatial resolution on SPECT quantification values. *J Nucl Med* 30: 508–514, 1989